

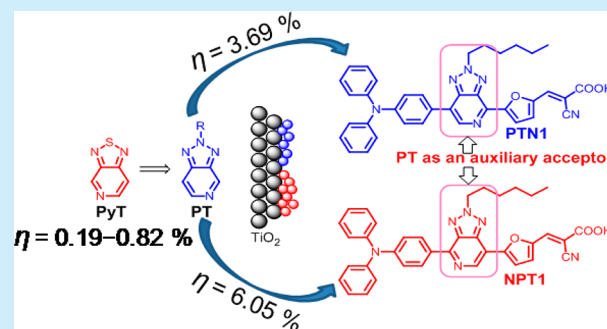
Incorporating a New 2*H*-[1,2,3]Triazolo[4,5-*c*]pyridine Moiety To Construct D–A– π –A Organic Sensitizers for High Performance Solar Cells

Sumit Chaurasia, Wei-I Hung, Hsien-Hsin Chou, and Jiann T. Lin*

Institute of Chemistry, Academia Sinica, 115 Nankang, Taipei, Taiwan

S Supporting Information

ABSTRACT: Two new organic dyes (PTN1 and NPT1) of the configuration D–A– π –A, based on 2*H*-[1,2,3]triazolo[4,5-*c*]pyridine (PT) as a central linker, have been synthesized and used as the sensitizers for dye-sensitized solar cells. Compared with pyridal[2,1,3]thiadiazole-containing congeners, the new dyes have conversion efficiencies nearly 1 order higher due to alleviation of charge trapping. The best conversion efficiency of the cell reaches 6.05% (under AM 1.5G irradiation). Upon addition of the coadsorbent CDCA, the efficiency is boosted to 6.76%, which reaches ~90% of the standard based on N719.



Organic dyes as light harvesters for dye-sensitized solar cells (DSSCs) have attracted considerable attention for the past two decades after the seminal report of Grätzel and co-workers on ruthenium complexes.¹ The record high conversion efficiency (η) of 13.0% has been achieved with a Zn-porphyrin complex-based DSSC recently.² In addition to ruthenium complexes and porphyrin dyes, metal-free sensitizers have also been intensively studied because of their molecular design flexibility and low cost.³ Very recently, an impressively high cell efficiency of 11.5% has also been achieved with a metal-free dye.^{3d}

A conventional metal-free dye has a common structural motif D– π –A,⁴ where D is the electron donor, A is the electron acceptor, and π is the conjugated spacer between the two. Charge transfer from the donor to the acceptor is beneficial to red shifting the absorption spectra and facilitating electron injection from the photoexcited dye molecule to the TiO₂ photoanode. In order to extend the absorption to a longer wavelength region for better light harvesting, the D– π –A design can be modified with insertion of an auxiliary acceptor, described as the D–A– π –A approach.⁵ High cell efficiencies up to 9% have been proven possible with D–A– π –A type sensitizers.⁶ In our earlier reports, we found that incorporation of electron deficient entities such as benzo[2,1,3]thiadiazole (BT) and the cyanovinyl entity in the conjugated spacer significantly red shift the absorption. However, we also found that charge trapping at the electron deficient unit of the spacer could jeopardize charge separation and result in inferior cell performance.⁷ Compared with the BT entity, dyes or polymers based on a benzotriazole (BTz) entity have a higher LUMO energy level and wider HOMO/LUMO gap,⁸ because the lone pair on the nitrogen atom of BTz is more basic than that on the sulfur atom of BT and hence is more easily donated into the

triazole ring,⁹ leading to the more electron-rich character of the BTz. Though the electron-withdrawing –N=N– and –C=N– groups¹⁰ render the BTz to be electron-accepting¹¹ and capable of electron transporting,¹² charge trapping is greatly alleviated in BTz-based dipolar sensitizers¹³ compared to the BT-based congeners.

In our previous report, we successfully synthesized a series of new dyes using an electron-deficient pyridal[2,1,3]thiadiazole¹⁴ (PyT) entity as an auxiliary acceptor and obtained the maximum efficiency of 4.24%. Though PyT dyes had an even longer wavelength absorption compared with their BTz congeners, they exhibited significant charge trapping and deteriorated the cell performance. Therefore, we decided to replace PyT with a 2*H*-[1,2,3]triazolo[4,5-*c*]pyridine (PT) entity so as to reach a compromise between light harvesting and charge trapping. To the best of our knowledge, there is no report on PT-based sensitizers for DSSCs. Herein, we report the synthesis and DSSC performance of two new PT-based organic dyes PTN1 and NPT1 for the first time. The power conversion efficiency up to 6.76% along with a high V_{OC} (0.70 V) was achieved with NPT1-based DSSC.

Our synthetic approach to regioregular PT-containing dyes is centered on the chemistry of 2*H*-[1,2,3]triazolo[4,5-*c*]pyridine (PT). The key precursor, 4,7-dibromo-2-hexyl-2*H*-[1,2,3]triazolo[4,5-*c*]pyridine (PTBr₂, **1**), was synthesized in two steps by following a modified reported method.¹⁵ The alkyl chain present at the nitrogen atom is beneficial to the solubility in common organic solvents and may possibly suppress the close contact of the electrolytes toward the TiO₂ surface (vide infra).¹⁶ The first Stille coupling of the asymmetric PTBr₂

Received: April 22, 2014

Published: May 22, 2014

selectively occurred at the position adjacent to the nitrogen.¹⁷ Consequently, two isomers (Figure 1), PTN1 (N atom facing

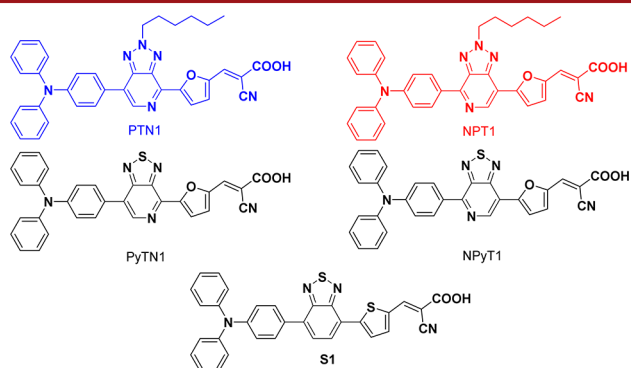
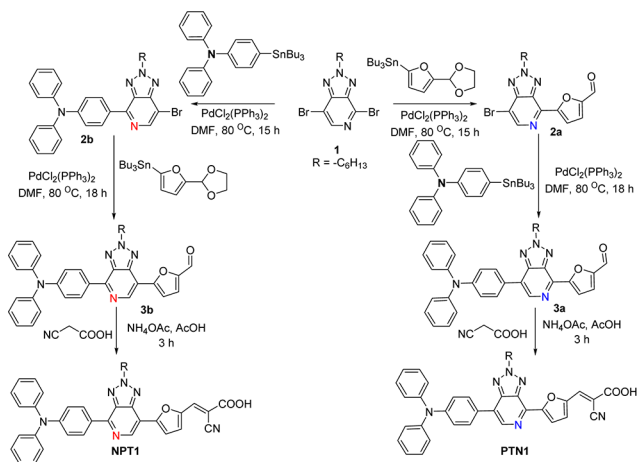


Figure 1. Structures of the dyes.

toward the acceptor) and NPT1 (N atom facing away from the acceptor), were successfully synthesized by following the pathways described in Scheme 1. The new dyes were characterized through ¹H, ¹³C NMR, and HRMS spectroscopy.

Scheme 1. Synthetic Scheme for PTN1 and NPT1 Dyes



UV-vis absorption spectra of both dyes in THF are presented in Figure 2, and their corresponding data are summarized in Table 1. The absorption spectra of both show two prominent bands in the regions 350–400 nm and 400–550

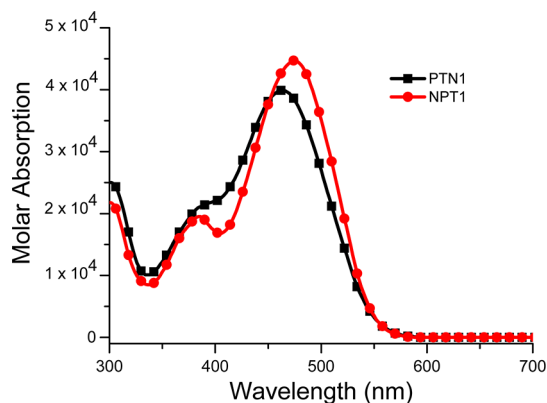


Figure 2. UV-vis absorption spectra of dyes in THF (10^{-5} M).

Table 1. Electro-optical Parameters of the Dyes

dyes	λ_{abs}^a ($\epsilon \times 10^4$ M ⁻¹ cm ⁻¹) ^a [nm]	λ_{max}^b [nm]	$E_{1/2}^c$ (ox) ^c [mV]	HOMO/ LUMO ^d [eV]	E_{0-0}^e [eV]	E_{0-0}^{*f} [V]
PTN1	464 (3.99), 390 (2.14)	482	548 (90)	5.75/- 3.37	2.38	-1.11
NPT1	476 (4.47), 386 (1.95)	476	553 (83)	5.75/- 3.38	2.37	-1.06

^aMeasured in THF (solution). ^bAbsorption maxima of film (adsorbed on TiO₂). ^cMeasured in CH₂Cl₂, scan rate = 100 mV s⁻¹; electrolyte = [(n-C₄H₉)₄][NPF₆]; $E_{\text{ox}} = (E_{\text{pa}} + E_{\text{pc}})/2$, $\Delta E_{\text{p}} = (E_{\text{pa}} - E_{\text{pc}})$ where E_{pa} and E_{pc} are peak anodic and cathodic potentials, respectively. Oxidation potential reported is adjusted to the potential of ferrocene which was used as an internal reference. ^dHOMO and LUMO energies are calculated using formula HOMO = 5.2 + ($E_{1/2} - E_{\text{Fc}}$), LUMO = $E_{0-0} - \text{HOMO}$. ^eOptical band gap energy gap, E_{0-0} , was derived from the intersection of absorption and emission spectra. ^f E_{0-0}^* : the excited state oxidation potential vs NHE.

nm. The former can be attributed to the aromatic $\pi-\pi^*$ transition of triphenylamine, and the later broad band can be attributed to the intramolecular charge transfer (ICT) from the triphenylamine donor to the cyanoacetic acid acceptor with some delocalized $\pi-\pi^*$ transition character.¹⁸ The λ_{max} value of the ICT band is 464 and 476 nm for PTN1 and NPT1, respectively. As expected, the absorption maxima of PT-based dyes are significantly blue-shifted (50–60 nm) compared with the PyT-based dyes,¹⁴ which can be attributed to the higher basicity of the nitrogen atom of the PT unit. This observation is in conformity with the trend found in benzotriazole- and benzothiadiazole-based dyes and is also supported by theoretical computations (vide infra).^{13a} It is noteworthy that the ICT band of PT-based dyes have much higher molar extinction coefficient (PTN1: 39900, NPT1: 44700) than PyT based dyes (SC-PyTN1: 19300, SC-NPyT1: 35100), implying a stronger $\pi-\pi^*$ transition character in the former and can be attributed to the better planarity of the conjugated spacer in the former (vide infra).

Figure S5 depicts the absorption spectra of the organic dyes adsorbed on a porous TiO₂ nanoparticle film (4 μm in thickness). Upon adsorption on the TiO₂, the dyes PTN1 and NPT1 exhibited a red shift of 18 nm and ~ 0 nm, respectively, indicating that J-aggregation of the dye molecules is less serious for the NPT1 dye and is evidenced from its higher cell efficiency (vide infra).

Electrochemical properties of PTN1 and NPT1 were studied by cyclic voltammetry (CV) in CH₂Cl₂ solutions. The cyclic voltammograms are shown in Figure S1, and the relevant data are compiled in Table 1. The dyes exhibit a reversible one-electron redox couple attributed to the oxidation of the arylamine. The NPT1 is oxidized at a higher potential than PTN1 due to the shorter distance between the electronegative nitrogen atom of PT and the arylamine in the former, similar to the trend observed in the PyT-based dyes.¹⁴ The HOMO energy level deduced from the redox potentials for PTN1 and NPT1 were found to be the same (5.75 eV), similar to the trend found in the PyT dyes.¹⁴ The excited state potential (E_{0-0}^*), estimated from the first oxidation potential at the ground state and E_{0-0} , are more negative (Table 1) than the conduction band edge of TiO₂ (-0.5 V vs NHE), ensuring an efficient electron injection process from the excited state of the dyes into the TiO₂ electrode. In contrast, the more positive oxidation potential of the dyes compared with that of the I⁻/I³⁻

redox couples (~ 0.4 V vs NHE) indicates that regeneration of the dyes is thermodynamically feasible.

The charge excitation behavior for the dyes is further examined via density functional calculations. Selected frontier orbitals of the dyes are shown in Figure 3. The results from the

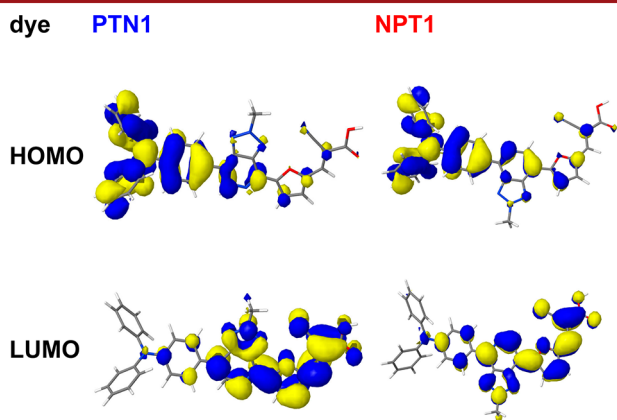


Figure 3. Frontier orbitals of the dyes (HOMO and LUMO).

time independent approach are compiled in Table S1. The HOMO is mainly distributed from the arylamine extending to the conjugated bridge. In comparison, the LUMO is mainly distributed from the 2-cyanoacrylic acid extending to the bridge. Therefore, charge transfer from the arylamine donor to the 2-cyanoacrylic acid acceptor is evident. Figure S4 displays the changes in the Mulliken charge for the dyes upon vertical excitation, as calculated via TDDFT (data Table S1, Supporting Information). Compared with the PyT unit in PyTN1 and NPyT1 dyes¹⁴ as well as BT unit in the S1 dye,^{7a} the Mulliken charge change (Δq) and the product of the oscillator strength and the Mulliken charge change ($f \times \Delta q$) of the PT unit in both PTN1 and NPT1 dyes for $S_0 \rightarrow S_1$ transition are less negative, indicating the charge trapping effect of the PT unit in both PTN1 and NPT1 dyes is alleviated significantly. In our previous report,¹⁹ we found that the more negative $f \times \Delta q$ value of the acceptor (anchor) could be used as an approximation for the electronic coupling strength from the dye molecule to the attached TiO₂ nanoparticle, and the more negative $f \times \Delta q$ value was corresponding with the larger short-circuit current of the cell. In this study, we also found that the acceptor of the new dyes had a more negative $f \times \Delta q$ value in the $S_0 \rightarrow S_1$ transition (PTN1: -0.20 ; NPT1: -0.23) compared with PyTN1 (-0.08) and NPyT1 (-0.02) dyes, and thus larger J_{SC} values (PTN1: 9.32; NPyT1: 13.37; PyTN1: 0.72; NPT1: 2.41 mA cm⁻²).

Dye-sensitized solar cells with an effective area of 0.16 cm² and the electrolyte composed of 0.05 M I₂/0.5 M LiI/0.5 M *tert*-butylpyridine (TBP) in acetonitrile solution were fabricated to explore the potentials of new dyes as the sensitizers. The incident photo-to-current conversion efficiency (IPCE) plots of the cells and the typical photocurrent–voltage J – V curves of the devices under the illumination of AM 1.5G (100 mW cm⁻²) as well as the dark current are shown in Figure 4. The performance parameters for the cells are summarized in Table 2. The highest IPCE performance was observed for the dye NPT1 in the range 350 to 650 nm, with a maximum value of $\sim 75\%$ at 520 nm ($\sim 85\%$ for NPT1 + 30 mM CDCA; see Figures 4b and S9). The power conversion efficiency of the cell is 3.69% and 6.05% for PTN1 and NPT1, respectively. In contrast, PyTN1 (0.19%) and NPyT1 (0.82%) have much

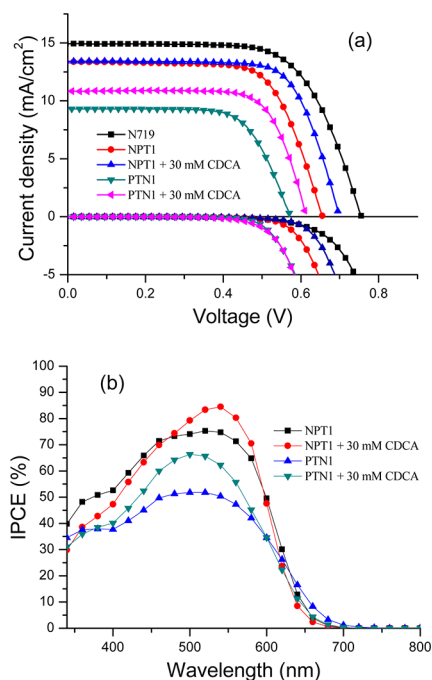


Figure 4. Current density–voltage/dark-current curves (a) and IPCE plots (b) of DSSCs based on PTN1 and NPT1 dyes.

Table 2. Device Performance Parameters of the Dyes

dyes	V_{OC}/V	$J_{SC}/\text{mA}/\text{cm}^2$	FF	η %
PTN1	0.57	9.32	0.70	3.69
PTN1 ^a	0.61	10.83	0.73	4.85
NPT1 ^b	0.66 ± 0.00	13.37 ± 0.31	0.69 ± 0.01	6.05 ± 0.15
NPT1 ^a	0.70	13.41	0.72	6.76
N719	0.76	13.93	0.66	7.53

^aDye with addition of 30 mM CDCA. ^bTaken from three measurements.

lower cell efficiencies.¹⁴ The short-circuit current (J_{SC}) value of the PT cells (PTN1: 9.32; NPT1: 13.37 mA cm⁻²) is also much higher than that of the PyT cells (PyTN1: 0.72; NPyT1: 2.41 mA cm⁻²). The nearly 1 order improvement of the efficiency and significantly higher J_{SC} value from PyT dyes to PT dyes can be attributed to serious charge trapping in the former (vide infra, see computation). It is interesting to note that the cell performance of NPT1 is much better than that of PTN1. This outcome could be ascribed to several reasons: (1) NPT1 has more intense ICT absorption; (2) NPT1 has a higher dye loading by $\sim 18\%$ (PTN1: 3.12×10^{-7} mol/cm² and NPT1: 3.68×10^{-7} mol/cm²); (3) NPT1 can suppress the dark current more effectively (vide infra, see electrochemical impedance spectra (EIS)); (4) there is better electron transport in the cell of NPT1 (vide infra, see EIS).

Although the long alkyl chain at the PT entity may help to ease dye aggregation,¹⁶ some degree of dye aggregation still occurs (Figure S5). As dye aggregation tends to quench the excited dye molecule and jeopardizes the electron injection efficiency,²⁰ we also fabricated DSSCs from the dyes containing 30 mM of chenodeoxycholic acid (CDCA) as the coadsorbent. The cell performance was improved significantly for both dyes: NPT1, 0.72 V, 10.63 mA cm⁻², 6.76%; PTN1, 0.61 V, 10.83 mA cm⁻², 4.85%. It is believed that both dye aggregation and charge recombination are eased. Alleviation of dye aggregation

can be supported by the blue shift of the absorption spectra of PTN1 and NPT1 when CDCA was added (Figure S5). Dark current suppression, on the other hand, is supported by comparison of EIS with and without addition of CDCA (vide infra, EIS).

Figure S6 shows the EIS of DSSCs measured in the dark. The intermediate frequency semicircle in the Nyquist plot represents the charge transfer phenomena between the TiO₂ surface and the electrolyte, i.e., the dark current. The resistance toward the dark current is larger for the cell of NPT1, indicating its more effective suppression of dark current. This is consistent with the smaller dark current (Figure 4a) and the larger V_{OC} (Table 2) measured. More compact packing of the NPT1 dye likely more efficiently blocks the electrolytes from approaching the TiO₂ surface. EIS was also measured for DSSCs of NPT1 with different concentrations of CDCA (0, 10, and 30 mM). The resistance toward the dark current increases as the concentration of CDCA increases (Figure S7).

Figure S8 shows the Nyquist plots upon illumination of 100 mW cm⁻² under open-circuit conditions. The radius of the intermediate frequency semicircle in the Nyquist plot will be used to deduce the electron-transport resistance, and the smaller radius means lower electron transport resistance. There is no significant difference found in the electron transport resistance between PTN1 (12.85 Ohm) and NPT1 (12.27 Ohm).

In summary, we have successfully designed and synthesized two new organic sensitizers (PTN1 and NPT1) containing 2H-[1,2,3]triazolo[4,5-c]pyridine as the central linkage for high-performance dye-sensitized solar cells. Compared to pyridal-[2,1,3]thiadiazole-based dyes, the conversion efficiency of the DSSCs is nearly 1 order higher. The best cell performance has a V_{OC} of 0.66 V, J_{SC} of 13.37 mA/cm², and conversion efficiency of 6.05%. Upon CDCA addition, the efficiency was further boosted to 6.76% reaching ~90% of the standard cell based on N719. Significant improvement of the cell performance of the new dyes compared to their pyridal[2,1,3]thiadiazole congeners can be attributed to the alleviation of charge trapping of the [1,2,3]triazolo[4,5-c]pyridine moiety compared with the pyridal[2,1,3]thiadiazole moiety.

■ ASSOCIATED CONTENT

Supporting Information

Experimental procedures and full spectroscopic data for all new dyes. This material is available free of charge via the Internet at <http://pubs.acs.org>.

■ AUTHOR INFORMATION

Corresponding Author

*E-mail: jtlin@gate.sinica.edu.tw.

Notes

The authors declare no competing financial interest.

■ ACKNOWLEDGMENTS

We thank the Academia Sinica and Ministry of Science and Technology, Taiwan, for financial support, and the Instrumental Center of Institute of Chemistry (AS).

■ REFERENCES

(1) O'Regan, B.; Grätzel, M. *Nature* **1991**, *353*, 737–740.

(2) Mathew, S.; Yella, A.; Gao, P.; Humphrey-Baker, R.; Curchod, B. F. E.; Ashari-Astani, N.; Tavernelli, I.; Rothlisberger, U.; Nazeeruddin, M. K.; Grätzel, M. *Nat. Chem.* **2014**, *6*, 242–247.

(3) (a) Grätzel, M. *Acc. Chem. Res.* **2009**, *42*, 1788–1798. (b) Hagfeldt, A.; Boschloo, G.; Sun, L. C.; Kloo, L.; Pettersson, H. *Chem. Rev.* **2010**, *110*, 6595–6663. (c) Ning, Z.; Fu, Y.; Tian, H. *Energy Environ. Sci.* **2010**, *3*, 1170–1181. (d) Zhang, M.; Wang, Y.; Xu, M.; Ma, W.; Li, R.; Wang, P. *Energy Environ. Sci.* **2013**, *6*, 2944–2949.

(4) (a) Mishra, A.; Fischer, M. K. R.; Bauerle, P. *Angew. Chem., Int. Ed.* **2009**, *48*, 2474–2499. (b) Hagfeldt, A.; Boschloo, G.; Sun, L.; Kloo, L.; Pettersson, H. *Chem. Rev.* **2010**, *110*, 6595–6663. (c) Yen, Y.-S.; Chou, H.-H.; Chen, Y.-C.; Hsu, C.-Y.; Lin, J. T. *J. Mater. Chem.* **2012**, *22*, 8374–8747. (d) Zhou, H.; Yang, L.; Stuart, A. C.; Price, S. C.; Liu, S.; You, W. *Angew. Chem., Int. Ed.* **2011**, *50*, 2995–2998. (e) Zhang, S.; Yang, X.; Numata, Y.; Han, L. *Energy Environ. Sci.* **2013**, *6*, 1443–1464.

(5) Wu, Y.; Zhu, W. *Chem. Soc. Rev.* **2013**, *42*, 2039–2058.

(6) (a) Qu, S.; Qin, C.; Islam, A.; Wu, Y.; Zhu, W.; Hua, J.; Tian, H.; Han, L. *Chem. Commun.* **2012**, *48*, 6972–6974. (b) Pei, K.; Wu, Y.; Islam, A.; Zhang, Q.; Han, L.; Tian, H.; Zhu, W. *ACS Appl. Mater. Interfaces* **2013**, *5*, 4986–4995.

(7) (a) Velusamy, M.; Thomas, K. R. J.; Lin, J. T.; Hsu, Y.-C.; Ho, K.-C. *Org. Lett.* **2005**, *7*, 1899–1902. (b) Chou, H.-H.; Chen, Y.-C.; Huang, H.-J.; Lee, T.-H.; Lin, J. T.; Tsai, C.; Chen, K. *J. Mater. Chem.* **2012**, *22*, 10929–10938. (c) Lin, R. Y.-Y.; Lee, C.-P.; Chen, Y.-C.; Peng, J.-D.; Chu, T.-C.; Chou, H.-H.; Yang, H.-M.; Lin, J. T.; Ho, K.-C. *Chem. Commun.* **2012**, *48*, 12071–12073.

(8) Zhang, Z. H.; Peng, B.; Liu, B.; Pan, C. Y.; Li, Y. F.; He, Y. H.; Zhou, K. H.; Zou, Y. P. *Polym. Chem.* **2010**, *1*, 1441–1447.

(9) Price, S. C.; Stuart, A. C.; Yang, L. Q.; Zhou, H. X.; You, W. *J. Am. Chem. Soc.* **2011**, *133*, 4625–4631.

(10) Newkome, G. R.; Paudler, W. W. *Contemporary Heterocyclic Chemistry*; John Wiley: New York, 1982.

(11) Palmer, M. H.; Simpson, I.; Wheeler, J. R. *Z. Naturforsch.* **1981**, *36a*, 1246–1252.

(12) Ahn, S.-H.; Czae, M.-Z.; Kim, E.-R.; Lee, H.; Han, S.-H.; Noh, J.; Hara, M. *Macromolecules* **2001**, *34*, 2522–2527.

(13) (a) Yen, Y.-S.; Lee, C.-T.; Hsu, C.-Y.; Chou, H.-H.; Chen, Y.-C.; Lin, J. T. *Chem.—Asian J.* **2013**, *8*, 809–816. (b) Mao, J.; Guo, F.; Ying, W.; Wu, W.; Li, J.; Hua, J. *Chem.—Asian J.* **2012**, *7*, 982–991.

(14) Chaurasia, S.; Hsu, C.-Y.; Chou, H.-H.; Lin, J. T. *Org. Electron.* **2014**, *15*, 378–390.

(15) (a) Tanimoto, A.; Yamamoto, T. *Adv. Synth. Catal.* **2004**, *346*, 1818–1823. (b) Patel, D. G. (Dan); Feng, F.; Ohnishi, Y.-y.; Abboud, K. A.; Hirata, S.; Schanze, K. S.; Reynolds, J. R. *J. Am. Chem. Soc.* **2012**, *134*, 2599–2612.

(16) Cui, Y.; Wu, Y.; Lu, X.; Zhang, X.; Zhou, G.; Miapheh, F. B.; Zhu, W.; Wang, Z.-S. *Chem. Mater.* **2011**, *23*, 4394–4401.

(17) Handy, S. T.; Wilson, T.; Muth, A. J. *Org. Chem.* **2007**, *72*, 8496–8500.

(18) Yang, H. Y.; Yen, Y. S.; Hsu, Y. C.; Chou, H.-H.; Lin, J. T. *Org. Lett.* **2010**, *12*, 16–19.

(19) Huang, S.-T.; Hsu, Y.-C.; Yen, Y.-S.; Chou, H.-H.; Lin, J. T.; Chang, C.-W.; Hsu, C.-P.; Tsai, C.; Yin, D.-J. *J. Phys. Chem. C* **2008**, *112*, 19739–19747.

(20) (a) Hara, K.; Sato, T.; Katoh, R.; Furube, A.; Ohga, Y.; Shinpo, A.; Suga, S.; Sayama, K.; Sugihara, H.; Arakawa, H. *J. Phys. Chem. B* **2003**, *107*, 597–606. (b) Hara, K.; Tchibana, Y.; Ohga, Y.; Shinpo, A.; Suga, S.; Sayama, K.; Sugihara, H.; Arakawa, H. *Sol. Energy Mater. Sol. Cells* **2003**, *77*, 89–103.